Frontiers in Mechanochemistry and Mechanical Alloying

INCOME2008
1-4 December, 2008

CRYSTALLITE SIZE DEPENDENT CATION DISTRIBUTION IN NANOSTRUCTURED SPINELS STUDIED BY NMR, MÖSSBAUER SPECTROSCOPY AND XPS

V. Šepelák[1,2ξ], I. Bergmann[3], S. Indris[1], P. Heitjans[4], K.D. Becker[5]
[1]Institute of Nanotechnology, Karlsruhe Institute of Technology, Karlsruhe, Germany
[2]Slovak Academy of Sciences, Košice, Slovakia
[3]Volkswagen AG, Wolfsburg, Germany
[4]Institute of Physical Chemistry and Electrochemistry, Leibniz University Hannover, Hannover, Germany
[5]Institute of Physical and Theoretical Chemistry, Braunschweig University of Technology, Braunschweig, Germany

Keywords: Spinel nanooxide, Cation distribution, NMR, Mössbauer spectroscopy, XPS

Abstract

Owing to the structural flexibility of spinels, providing a wide range of physical and chemical behavior, these materials have been considered as a convenient model system for the investigation of the size dependent properties of complex ionic systems. In this work, quantitative information is obtained on the crystallite size dependent ionic configuration in nanosized spinel oxides prepared by mechanochemical processing of the corresponding bulk materials. Experimentally determined values of the crystallite size and of the mean degree of inversion of nanostructured spinels are used to calculate the volume fraction of interfaces/surfaces and their thickness in the nanomaterials.

Introduction

Nanocrystalline complex oxides are an important class of nanostructured materials that attract special attention, for example, as advanced ceramics, magnetics, ferroelectrics, ferroelastics, superconductors, sensors, actuators, pigments, refractories, catalysts and sorbents. The mechanochemical routes provide an opportunity to fabricate novel nanostructured oxides with anomalous properties markedly different from those of their bulk-sized counterparts prepared by the standard processing [1-3]. However, precise knowledge of the relationships between particle shape and size, interior and surface structures, and the resulting properties of these nanomaterials is still lacking.

In this work, the crystallite size dependent cation distribution in $MgAl_2O_4$, $Li_{0.5}Fe_{2.5}O_4$ and $ZnFe_2O_4$ spinel oxides is studied by ^{27}Al magic angle spinning (MAS) nuclear magnetic resonance (NMR), ^{57}Fe Mössbauer spectroscopy and X-ray photoelectron spectroscopy (XPS), respectively. Both $MgAl_2O_4$ and $ZnFe_2O_4$ belong to the group of 2-3 spinels of the

$$M1^{2+}M2_2^{3+}O_4 \quad \text{type,}$$

whereas $Li_{0.5}Fe_{2.5}O_4$ is a 1-3 spinel of the type,

$$M1_{0.5}^{1+}M2_{2.5}^{3+}O_4$$

where 2-3 and 1-3 refer to the valences of $M1$ and $M2$ cations. Despite their deceptively simple structure, many spinel oxides exhibit complex disordering phenomena involving the redistribution of $M1$ and $M2$ cations over the sites of tetrahedral (A) and octahedral [B] coordination. To emphasize the site occupancy at the atomic level, the structural formulas of these materials may be written as $(M1_{1-\lambda}M2_{\lambda})[M1_{\lambda}M2_{2-\lambda}]O_4$ (for 2-3 spinels) and $(M1_{1-\lambda}M2_{\lambda})[M1_{\lambda-0.5}M2_{2.5-\lambda}]O_4$ (for 1-3 spinels), where parentheses and square brackets denote (A) and [B] sites, respectively. The symbol λ represents the so-called degree of inversion defined as the fraction of the (A) sites occupied by trivalent ($M2^{3+}$) cations. For 2-3 spinels, it varies from $\lambda = 0$ (normal spinel) to $\lambda = 1$ (fully inverse spinel), whereas λ takes a value from 0.5 to 1 in the case of 1-3 spinels. The values of $\lambda_s = 2/3$ and $\lambda_s = 5/6$ correspond to the random arrangement of cations in 2-3 and 1-3 spinels, respectively.

Experimental

Nanocrystalline $MgAl_2O_4$, $Li_{0.5}Fe_{2.5}O_4$ and $ZnFe_2O_4$ were prepared by high-energy milling of coarse high-purity spinels synthesized by a conventional ceramic route (for details, see Refs. [4-6]).

^{27}Al MAS NMR spectra were recorded at room temperature using a Bruker MSL 400 spectrometer at a spinning rate of 15 kHz. An external magnetic field of 9.4 T was applied, corresponding to a ^{27}Al resonance frequency of 104.2 MHz. The ^{27}Al chemical shifts are referenced to an 1 M $Al(NO_3)_3$ aqueous solution. The low-temperature (5 K) Mössbauer spectra of $Li_{0.5}Fe_{2.5}O_4$ were taken in transmission geometry at zero applied magnetic field and at an external magnetic field of 5.5 T applied perpendicular to the γ-ray direction. A ^{57}Co/Rh γ-ray source was used. The velocity scale was calibrated relative to ^{57}Fe in Rh. XPS measurements were performed at room temperature with an ESCALAB 220iXL spectrometer (Fisons Instruments). The degree of inversion, λ, was calculated from the intensity ratio of the spectral components corresponding to (A)- and [B]-site cations, according to formulas $\lambda = 2I_{(A)}/(I_{(A)}+I_{[B]})$ and $\lambda = 2.5I_{(A)}/(I_{(A)}+I_{[B]})$ for 2-3 and 1-3 spinels, respectively.

ξ email : vladimir.sepelak@kit.edu

Results

Figure 1 shows room-temperature ^{27}Al MAS NMR spectra of $MgAl_2O_4$ milled for various times. During the high-energy milling process, the material is subjected to a continuous fragmentation accompanied by the crystallite size reduction to the nanometer range and by an increase of the volume fraction of interfaces/surfaces. With increasing milling time, the average crystallite size (D) of $MgAl_2O_4$ monotonically decreases from D = 150 nm, reaching the value D = 8.1 nm after 2 h of milling. The NMR spectra of $MgAl_2O_4$, independently of its crystallite size, consist of two well-resolved peaks in the region characteristic of tetrahedrally coordinated aluminium, Al^{3+}(A), (chemical shift $\delta \approx$ 70 ppm) and octahedrally coordinated aluminium, Al^{3+}[B], ($\delta \approx$ 8 ppm) [7]. Note that, in contrast to the (A) site spectral component, the [B] site subspectrum exhibits two maxima. This could be due to an electric field gradient acting on Al^{3+}[B] nuclei arising from an asymmetric charge distribution around the [B] site (second-order quadrupole interaction) [8]. From the intensity ratio of the (A) and [B] spectral components, one can easily deduce quantitative information on the cation distribution in the material ($I_{(A)}/I_{[B]} = \lambda/(2-\lambda)$). The degree of inversion of bulk $MgAl_2O_4$ (D = 150 nm) was found to be λ_c = 0.23(3). This indicates that the bulk aluminate adopts a partly inverse spinel structure of the type $(Mg_{0.77}Al_{0.23})[Mg_{0.23}Al_{1.77}]O_4$. It is clearly visible that the reduction of the crystallite size of $MgAl_2O_4$ is accompanied by the redistribution of the intensities of the (A) and [B] spectral lines, reflecting a decrease of the concentration of Al^{3+} cations on [B] sites and, vice versa, an increase of the population of Al^{3+} ions on (A) sites. The important observation is that the degree of inversion of $MgAl_2O_4$ increases monotonically with decreasing D, reaching the value λ = 0.31(1) for crystallites with the size of 8.1 nm (Table 1). Thus, high-energy milling of $MgAl_2O_4$ induces a homogeneous mechanochemical reaction yielding a nonequilibrium cation distribution. The mechanically induced redistribution of Al^{3+} and Mg^{2+} cations between the two inequivalent spinel lattice sites in $MgAl_2O_4$ can be quantitatively described by the following reaction: $(Mg_{0.77}Al_{0.23})[Mg_{0.23}Al_{1.77}]O_4 \rightarrow (Mg_{0.69}Al_{0.31})[Mg_{0.31}Al_{1.69}]O_4$ [4].

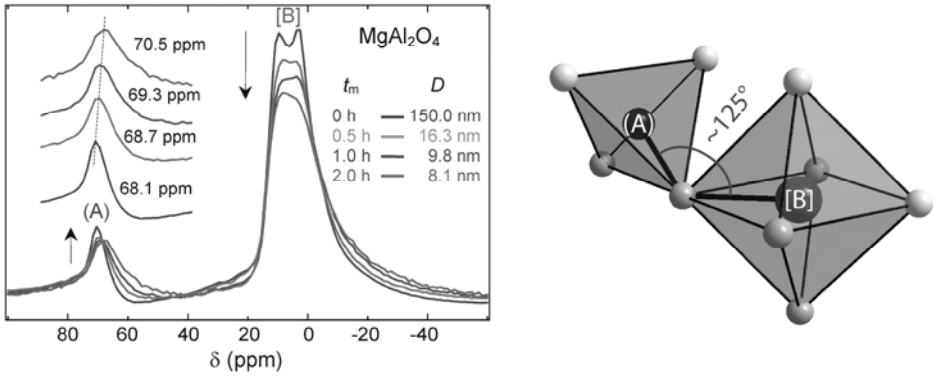

Figure 1. ^{27}Al MAS NMR spectra of $MgAl_2O_4$ milled for various times. The milling times (t_m) and the corresponding crystallite sizes (D) are shown in the figure. (A) and [B] denote tetrahedrally and octahedrally coordinated Al^{3+} cations, respectively. Arrows emphasize the redistribution of the (A) and [B] spectral intensities. The inset shows the shift of the (A) spectral line.

Table 1. The volume fraction of interfaces/surfaces (w) and their thickness (t) in nanocrystalline spinel oxides estimated using the experimentally determined mean degree of inversion (λ) and the average crystallite diameter (D). It was taken into account that nanosized crystallites (grains) in oxides possess the cation ordered bulk-like structure characterized by the degree of inversion λ_c, whereas the interfaces/surfaces are disordered due to the random distribution of cations (λ_s).

Spinel	D (nm)	λ	λ_c	λ_s	w (%)	t (nm)
$MgAl_2O_4$	8.1	0.31	0.23	2/3	18.3	0.3
$Li_{0.5}Fe_{2.5}O_4$	8.0	0.90	1.00	5/6	60.0	1.1
$ZnFe_2O_4$	10.0	0.41	0.00	2/3	61.5	1.4

$\lambda = 2I_{(A)}/(I_{(A)}+I_{[B]})$ for 2-3 spinels; $\lambda = 2.5I_{(A)}/(I_{(A)}+I_{[B]})$ for 1-3 spinels.

$w = 100[(\lambda-\lambda_c)/(\lambda_s-\lambda_c)]$.

$t = D/2-[(D/2)^3(100-w)/100]^{1/3}$.

The interesting observation is that the crystallite size reduction of the spinel aluminate brings about both a noticeable broadening and a shift (towards negative chemical shifts) of the (A) and [B] NMR spectral lines (see inset of Fig. 1), implying a change in the local atomic environments of Al^{3+}(A) and Al^{3+}[B] ions. This variation may be explained by the presence of deformed AlO_6 octahedra and AlO_4 tetrahedra [6, 9] in the interface/surface regions of nanostructured spinel.

To study the size dependent cation distribution in $Li_{0.5}Fe_{2.5}O_4$, we found it necessary to perform low-temperature ^{57}Fe Mössbauer measurements in conjunction with large external magnetic fields (B_{ext}). Without application of B_{ext}, the local magnetic fields $B_{(A)}$ and $B_{[B]}$, acting on the iron nuclei in the (A) and [B] spinel sublattices, do not differ substantially. This is demonstrated in the Mössbauer spectrum of bulk $Li_{0.5}Fe_{2.5}O_4$ (Fig. 2(a)), where the (A) and [B] subspectra are difficult to resolve because of strongly overlapping lines. Note that in the case of a nanoscale spinel, the separation of the (A) and [B] subspectra is an even more difficult problem because the

hyperfine interactions in (A) and [B] sites additionally possess a more or less distributive character [10]. In the presence of an external magnetic field, B_{ext} adds to $B_{(A)}$ and subtracts from $B_{[B]}$ as a consequence of the antiparallel alignment of the spins of Fe^{3+} cations at (A) and [B] sites. Thus, the use of large external magnetic fields creates an effective separation of the overlapping subpatterns (Fig. 2(b)), thereby allowing for an accurate determination of the cation distribution. Simultaneous use of low temperatures further simplifies the evaluation of Mössbauer spectra, because it suppresses magnetic relaxation effects (collective magnetic excitations, superparamagnetism) associated with the nanoscale nature of mechanochemically prepared oxides [11]. The low-temperature (5 K) in-field (5.5 T) Mössbauer spectra with the completely resolved (A) and [B] subspectra for both bulk and nanoscale milled $Li_{0.5}Fe_{2.5}O_4$ (Figs. 2(b) and 2(c)) demonstrate that the crystallite size reduction caused by milling for 2 h results in a decrease of the concentration of Fe^{3+} cations on (A) sites and, vice versa, in an increase of the population of Fe^{3+} ions on [B] sites. Whereas the bulk ferrite (D = 120 nm) adopts the fully inverse spinel structure of $(Fe)[Li_{0.5}Fe_{1.5}]O_4$ (λ = 1.00(1)), the degree of inversion of nanosized $Li_{0.5}Fe_{2.5}O_4$ with D = 8.0 nm was found to be λ = 0.90(2). Thus, the crystal chemical formula emphasizing the site occupancy at the atomic level for nanocrystalline lithium ferrite can be written as $(Li_{0.1}Fe_{0.9})[Li_{0.4}Fe_{1.6}]O_4$ [5].

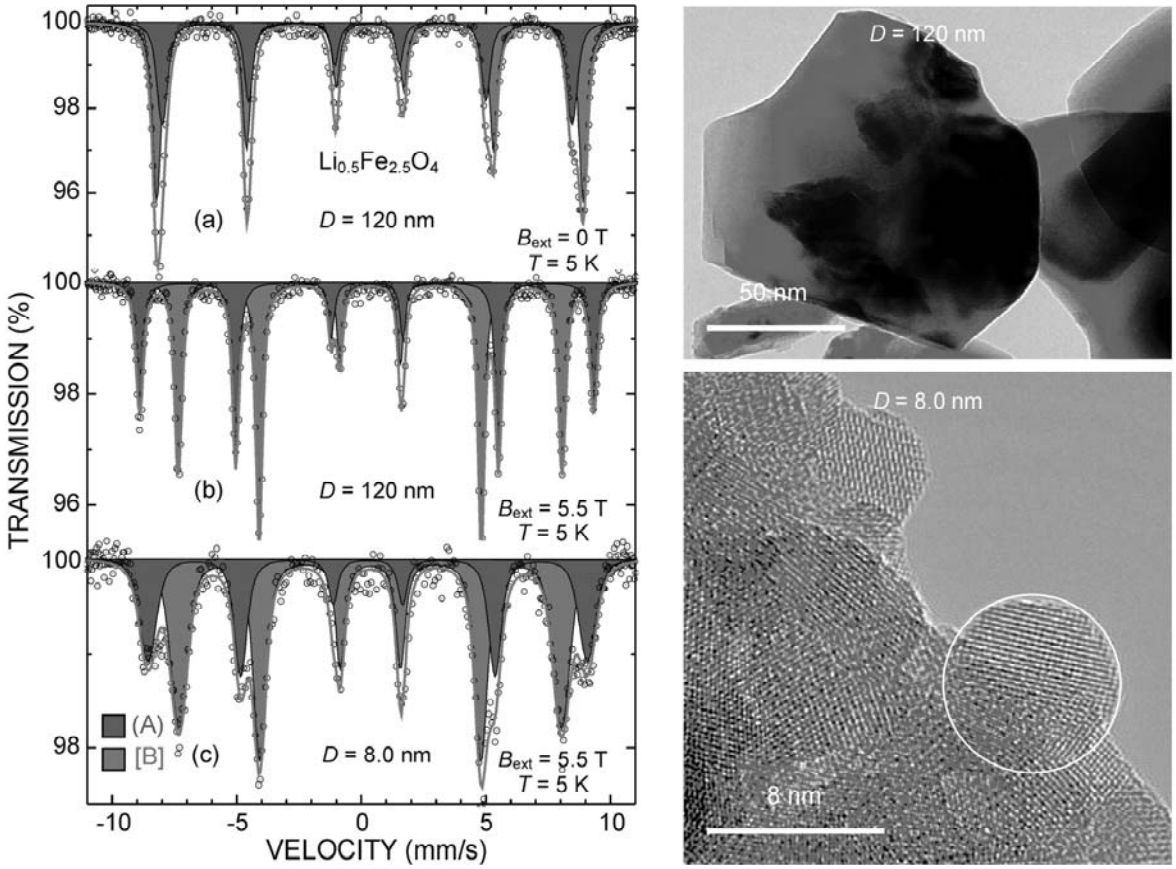

Figure 2. Low-temperature (5 K) ^{57}Fe Mössbauer spectra (left) and the corresponding TEM images (right) of bulk (D = 120 nm) and nanocrystalline (D = 8.0 nm) $Li_{0.5}Fe_{2.5}O_4$. The spectrum of the bulk material taken at zero applied magnetic field (a) shows strongly overlapping (A) and [B] lines. The in-field spectra of bulk (b) and nanocrystalline (c) $Li_{0.5}Fe_{2.5}O_4$ show completely resolved (A) and [B] subspectra.

It was found that mechanochemical processing of a normal spinel such as $ZnFe_2O_4$ is, contrary to the inverse spinel (e.g., $Li_{0.5}Fe_{2.5}O_4$), accompanied by an increase of the concentration of Fe^{3+} cations on (A) sites and, consequently, by an increase of the population of divalent metal cations on [B] sites [12-14]. This is clearly demonstrated in the XPS spectra of $ZnFe_2O_4$ milled for various times (Fig. 3). The Zn $2p_{3/2}$ signal of bulk $ZnFe_2O_4$ (D = 110 nm) consists of a single sharp peak located at 1021.8 eV (Fig. 3(a)), which corresponds to the tetrahedrally coordinated zinc ions [15]. This indicates that bulk $ZnFe_2O_4$ adopts the normal spinel structure (λ = 0). With increasing milling time (with decreasing D), the XPS signal becomes broader, and a new spectral component gradually appears on its right side (at 1023.2 eV), corresponding to octahedrally coordinated zinc [15]. Note that the new spectral component is clearly visible in the XPS spectrum of $ZnFe_2O_4$ already after 2

min of milling (Fig. 3(b)). After relatively short milling time (18 min), the concentration of Zn^{2+}[B] cations reaches the value of λ = 0.41(2); see Fig. 3(c). Thus, the nanocrystalline $ZnFe_2O_4$ with D = 10 nm exhibits a partly inverse spinel structure with the degree of inversion of about 0.41. This observation is consistent with the results of EXAFS investigations of nanoscale Zn-containing spinels [16, 17]. Quantitatively, the homogeneous mechanochemical process of cation redistribution in $ZnFe_2O_4$ can be formulated as
$(Zn)[Fe_2]O_4 \rightarrow (Zn_{0.59}Fe_{0.41})[Zn_{0.41}Fe_{1.59}]O_4$ [6].

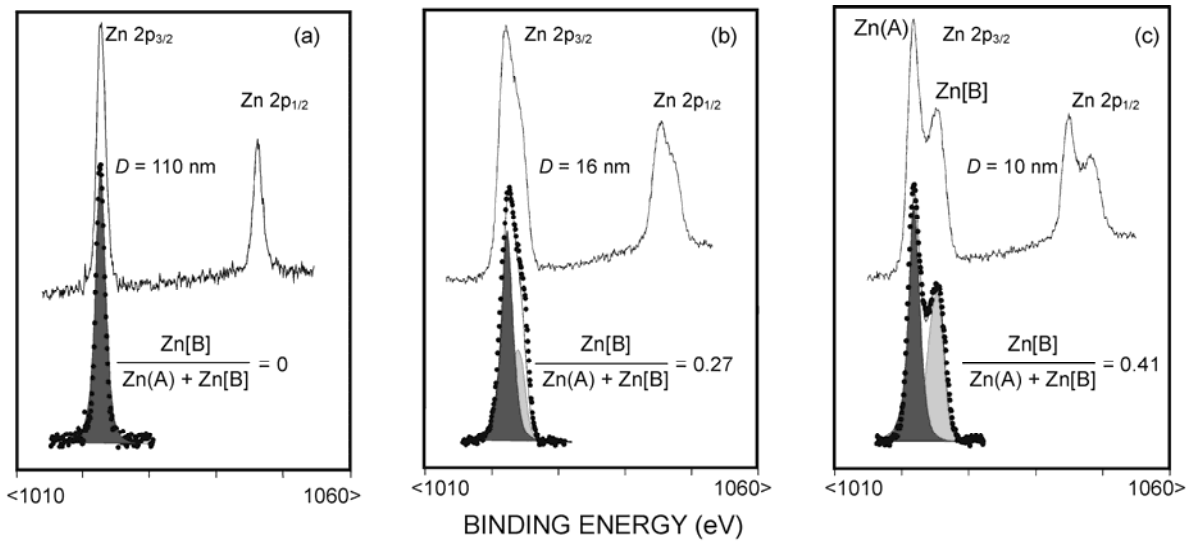

Figure 3. XPS spectra of unmilled $ZnFe_2O_4$ (a) and of $ZnFe_2O_4$ milled for 2 min (b) and 18 min (c). The corresponding crystallite sizes (D) are shown in the figure.

Discussion

It is well recognized that nanostructured oxides prepared by high-energy milling of bulk materials consist of crystallographically ordered regions (often called nanocrystalline grains or crystallites) surrounded by disordered internal interfaces (grain boundaries) and external surfaces (near-surface layers). The λ values of nanosized $MgAl_2O_4$, $Li_{0.5}Fe_{2.5}O_4$ and $ZnFe_2O_4$, determined in the present work by NMR, Mössbauer spectroscopy, and XPS (see Table 1), have therefore to be considered as mean values reflecting the cation distribution within the whole volume of the materials, i.e., within their ordered grains and disordered interfaces/surfaces. It was revealed in our work [18, 19] that the major feature of the atomic configuration in the interface/surface regions of nanocrystalline spinel oxides is a nonequilibrium ionic distribution characterized by the nearly random arrangement of cations. This is in contrast to the ordered grains of nanooxides, which were found to exhibit an equilibrium cation distribution. Thus, taking into account that grains in the nanocrystalline spinel oxides possess the same structure as the bulk materials (characterized by the degrees of inversion: λ_c = 0.23 for $MgAl_2O_4$, λ_c = 1 for $Li_{0.5}Fe_{2.5}O_4$ and λ_c = 0 for $ZnFe_2O_4$) and that the interfaces/surfaces are structurally disordered due to the random distribution of cations (λ_s = 2/3 for $MgAl_2O_4$ and $ZnFe_2O_4$, λ_s = 5/6 for $Li_{0.5}Fe_{2.5}O_4$), the experimentally determined λ values can be expressed as $\lambda = (1 - w)\lambda_c + w\lambda_s$, where w is the volume fraction of interfaces/surfaces in the nanocrystalline spinels. Assuming a spherical shape of nanocrystallites in the milled $MgAl_2O_4$, $Li_{0.5}Fe_{2.5}O_4$ and $ZnFe_2O_4$, we estimated the volume fraction of interfaces/surfaces and their thickness (t) using the experimentally determined λ, λ_c and D values (see Table 1). As can be seen, the fraction of cations located in the interface/surface regions of spinel nanooxides of comparable crystallite size (D ~ 10 nm) ranges from about 18 to 62%. The volume fraction of interfaces/surfaces in the relatively brittle spinel aluminate ($MgAl_2O_4$) was found to be smaller than that in spinel ferrites ($Li_{0.5}Fe_{2.5}O_4$, $ZnFe_2O_4$), which are generally more ductile materials. The estimated thickness of the interface/surface regions in nanocrystalline spinels extends up to 1.4 nm (Table 1). This value of the interface/surface thickness is in reasonable agreement with that estimated for other nanoscale spinel oxides [18-21]. We note that, in general, 1-2 nm is also a typical thickness of grain boundary regions in non-spinel oxides, such as nanocrystalline milled $LiNbO_3$ [22], where the grain boundaries were even shown to be amorphous.

Conclusions

Due to the ability of spectroscopic methods (NMR, Mössbauer spectroscopy, XPS) to discriminate between probe nuclei on the inequivalent crystallographic sites provided by the spinel structure, valuable insight into the crystallite size dependent cation distribution in spinels was obtained. It was revealed that mechanochemical processing of spinels, independently of their ionic configuration in the initial bulk state, induces a homogeneous reaction which tends to randomize cations among (A) and [B] lattice sites. Thus, for normal spinel ($ZnFe_2O_4$; λ = 0), partially inverse spinel ($MgAl_2O_4$; λ = 0.23) as well as for fully inverse spinel ($Li_{0.5}Fe_{2.5}O_4$; λ = 1), with decreasing crystallite size, the cation distribution was found to be directed

towards random arrangement. The cation order-disorder process was found to be accompanied by a deformation of polyhedron geometries. Taking into account that nanocrystalline spinel oxides prepared by mechanochemical route possess a nonuniform structure consisting of nanosized grains with an equilibrium cation distribution surrounded by the disordered interfaces/surfaces with the random arrangement of cations, the volume fraction of interfaces/surfaces and their thickness were estimated using the experimentally determined λ, λ_c and D values. The fraction of cations located in the interface/surface regions of spinel nanooxides of comparable crystallite size ($D \sim$ 10 nm) ranges from about 18 to 62%. The volume fraction of interfaces/surfaces in the relatively brittle spinel aluminate ($MgAl_2O_4$) was found to be smaller than that in spinel ferrites ($Li_{0.5}Fe_{2.5}O_4$, $ZnFe_2O_4$), which are generally more ductile materials. The thickness of the structurally disordered interface/surface regions in nanostructured spinels is estimated to extend up to 1.4 nm.

Acknowledgements

The present work was supported by the DFG, the APVV (Grant 0728-07), the VEGA (2/0065/08), and by the AvH Foundation.

References

1. V.V. Boldyrev, *Russ. Chem. Rev.*, 75 (2006) 177.
2. E. Avvakumov, M. Senna, and N. Kosova, *Soft Mechanochemical Synthesis: A Basis for New Chemical Technologies*, Kluwer Academic Publishers, Boston, (2001).
3. V. Šepelák, K.D. Becker, and Z.A. Munir (ed.), *Mechanochemistry and Mechanical Alloying 2003*, *J. Mater. Sci.*, 39 (2004) 4983.
4. V. Šepelák, S. Indris, I. Bergmann, A. Feldhoff, K.D. Becker, and P. Heitjans, *Solid State Ionics*, 177 (2006) 2487.
5. I. Bergmann, V. Šepelák, A. Feldhoff, P. Heitjans, and K.D. Becker, *Rev. Adv. Mater. Sci.*, 18 (2008) 375.
6. V. Šepelák, S. Indris, P. Heitjans, and K.D. Becker, *J. Alloy. Compd*., 434-435 (2007) 776.
7. R.L. Millard, R.C. Peterson, and B.K. Hunter, *Am. Mineral.*, 77 (1992) 44.
8. G. Engelhardt and D. Michel, *High Resolution Solid State NMR of Silicates and Zeolites*, John Wiley and Sons, Chichester, (1987).
9. N. Kashii, H. Maekawa, and Y. Hinatsu, *J. Am. Ceram. Soc.*, 82 (1999) 1844.
10. V. Šepelák, D. Baabe, F.J. Litterst, and K.D. Becker, *J. Appl. Phys.*, 88 (2000) 5884.
11. S. Mørup, in *Mössbauer Spectroscopy Applied to Inorganic Chemistry, Vol. 2*, (ed.) G.J. Long, Plenum Press, New York (1987), p. 89.
12. V. Šepelák, K. Tkáčová, V.V. Boldyrev, S. Wißmann, and K.D. Becker, *Physica B*, 234-236 (1997) 617.
13. V. Šepelák and K.D. Becker, *J. Mater. Synth. Proces.*, 8 (2000) 155.
14. C.N. Chinnasamy, A. Narayanasamy, N. Ponpandian, and K. Chattopadhyay, *Mater. Sci. Eng. A*, 304-306 (2001) 983.
15. P. Druska, U. Steinike, and V. Šepelák, *J. Solid State Chem.*, 146 (1999) 13.
16. N. Ponpandian, A. Narayanasamy, C.N. Chinnasamy, N. Sivakumar, J.M. Greneche, K. Chattopadhyay, K. Shinoda, B. Jeyadevan, and K. Tohji, *Appl. Phys. Lett.*, 86 (2005) 192510.
17. S.A. Oliver, V.G. Harris, H.H. Hamdeh, and J.C. Ho, *Appl. Phys. Lett.*, 76 (2000) 2761.
18. V. Šepelák, A. Feldhoff, P. Heitjans, F. Krumeich, D. Menzel, F.J. Litterst, I. Bergmann, and K.D. Becker, *Chem. Mater.*, 18 (2006) 3057.
19. V. Šepelák, I. Bergmann, A. Feldhoff, P. Heitjans, F. Krumeich, D. Menzel, F.J. Litterst, S.J. Campbell, and K.D. Becker, *J. Phys. Chem. C*., 111 (2007) 5026.
20. M. Muroi, R. Street, P.G. McCormick, and J. Amighian, *Phys. Rev. B*, 63 (2001) 184414.
21. Y.D. Zhang, S.H. Ge, H. Zhang, S. Hui, J.I. Budnick, W.A. Hines, M.J. Yacaman, and M. Miki, *J. Appl. Phys.*, 95 (2004) 7130.
22. P. Heitjans, M. Masoud, A. Feldhoff, and M. Wilkening, *Faraday Discuss.*, 134 (2007) 67.